Neuroradiology (2020) 62:455–461
https://doi.org/10.1007/s00234-019-02345-3

DIAGNOSTIC NEURORADIOLOGY

Silent MRA: arterial spin labeling magnetic resonant angiography with ultra-short time echo assessing cerebral arteriovenous malformation

Nobuhiko Arai[1] · Takenori Akiyama[1] · Kazuhiro Fujiwara[2] · Kazunari Koike[1] · Satoshi Takahashi[1] · Takashi Horiguchi[1] · Masahiro Jinzaki[2] · Kazunari Yoshida[1]

Received: 30 July 2019 / Accepted: 9 December 2019 / Published online: 3 January 2020

Abstract

Purpose MR angiography using the silent MR angiography algorithm (silent MRA), which combines arterial spin labeling and an ultrashort time echo, has not been used for the evaluation of cerebral arteriovenous malformations (CAVMs). We aimed to determine the usefulness of silent MRA for the evaluation of CAVMs.

Methods Twenty-nine CAVMs of 28 consecutive patients diagnosed by 4D CT angiography or digital subtraction angiography, who underwent both time-of-flight (TOF) MRA and silent MRA, were enrolled. Two observers independently assessed the TOF-MRA and silent MRA images of CAVMs. Micro AVM was defined as AVM with a nidus diameter less than 10 mm. The detection rate, visualization of the components, and accuracy of Spetzler–Martin grade were evaluated with statistical software R.

Results For all 29 CAVMs, 23 (79%) lesions were detected for TOF-MRA and all for silent MRA. Of 10 micro AVMs, only 4 (40%) lesions were detectable on TOF-MRA and all (100%) on silent MRA. The visibility of the nidus and drainer was significantly better for silent MRA than TOF-MRA ($p < 0.001$), while there was no significant difference in the feeder between the two sequences. The accuracy rates of the Spetzler–Martin grade for the TOF and silent MRA were 38% (11/29) and 79.3% (23/29), respectively ($p < 0.001$).

Conclusions Silent MRA is useful for evaluating CAVM components and detecting micro AVM.

Keywords Arteriovenous malformation · Magnetic resonance angiography · Arterial spin labeling · Time echo · AV shunt disease · Magnetic resonance imaging

Abbreviations

CAVM	Cerebral arteriovenous malformations
ARUBAA	Randomized trial of Unruptured Brain Arteriovenous malformations
DSA	Digital subtraction angiography
D	Dimensional
TOF	Time of flight
MRA	Magnetic resonance angiography
ASL	Arterial spin labeling
UTE	Ultrashort time echo
AV	Arteriovenous
T	Tesla
MRI	Magnetic resonance imaging
NEX	Number of excitations
MIP	Maximum intensity projection
PLD	Post-labeling delay

Introduction

Cerebral arteriovenous malformations (CAVMs) are congenital vascular abnormalities that connect arteries with veins, and they can cause fatal cerebral and subarachnoid hemorrhages [1, 2]. However, surgical treatment of CAVMs sometimes leads to serious complications, so clinicians tend to carefully consider the indications for surgery. A recently published randomized trial of unruptured brain arteriovenous

✉ Nobuhiko Arai
shinton0101@yahoo.co.jp

[1] Department of Neurosurgery, School of Medicine, Keio University, 35 Shinanomachi, Shinjuku, Tokyo, Japan

[2] Department of Radiology, Keio University Hospital, Shinjuku, Tokyo, Japan

malformations (the ARUBA study) just increased this tendency [3]. To help assess the risk of hemorrhage and to determine treatment strategies, imaging studies involving the detailed structures of CAVMs are required. The following factors have been reported as risk factors for cerebral hemorrhage due to CAVM surgery: history of hemorrhage, localization of nidus, aneurysm, location in a deep part of the derived vein, and high Spetzler–Martin grade [4–9].

To evaluate CAVMs, digital subtraction angiography (DSA) is the gold standard radiological technique. However, this method is not suitable for screening and follow-up of CAVMs in routine medical care because it can cause thromboembolic complications and involves contrast media and radiation exposure [10–12]. Therefore, 3D time of flight (TOF)-magnetic resonance angiography (MRA) is often used instead of DSA to follow up patients with CAVMs because of its less invasiveness. However, the method confers insufficient visualization of certain vascular components of CAVMs [13, 14], and cannot detect especially small lesions, which, for example, frequently occur in hereditary hemorrhagic telangiectasia (HHT) [15, 16].

MRA using the silent MRA algorithm (silent MRA), which combines arterial spin labeling (ASL) and an ultrashort time echo (UTE), was developed in 2012 [17]. Although ASL-based MRA has been reported to be useful in the evaluation of CAVMs [18–26], many studies were about ASL-based four-dimensional (4D) MRA techniques using different inversion time [18–21]. Silent MRA could only visualize a single time point which is very simple and approachable for clinicians. In addition, UTE techniques may have advantages over ASL-based 4D MRA because it minimizes dissipation of the labeled intracranial blood flow signal and alleviates magnetic susceptibility artifacts. To our knowledge, however, the usefulness of silent MRA in the evaluation of CAVMs has not been investigated. Therefore, this study aimed to determine whether silent MRA is useful for evaluating CAVMs.

Materials and methods

Study population

The study retrospectively recruited consecutive patients with CAVMs; The inclusion criteria were as follows: patients of all ages who were diagnosed by 4D CT angiography (CTA) or DSA, and who underwent the two types of MRA at Keio University hospital between August 2015 and August 2018. Of 37 CAVM patients who met the inclusion criteria, we excluded 4 patients who had a complete cure of AVMs on DSA after endovascular treatment and 5 patients whose TOF-MRA images did not cover whole parts of AVM. One patient had double lesions. Thus, 29 CAVMs of 28 patients were included in this study. The mean age of the patients was 47 years (range 15–78 years). The study population mostly included males (16/28). The mean Spetzler–Martin grade was 2.24 ± 0.95 (Grade 1, 10; Grade 2, 9; Grade 3, 8; Grade 4, 2; Grade5, 0). The mean size of CAVMs was 23.8 ± 19.1 mm (1.5–67 mm). Ten micro AVMs with a nidus diameter less than 10 mm were included, and 66% of patients were incidentally diagnosed (other presentations include: 5 cases, hemorrhage; 4 cases, epilepsy). Written informed consent was obtained from the patients or their families.

MRA technique

Three-dimensional TOF-MRA and silent MRA were performed on the same test day using a 3-T magnetic resonance imaging (MRI) system (SIGNA Pioneer; GE Healthcare, Milwaukee, Wisconsin) and a 24-channel head coil. The scan parameters of TOF-MRA were as follows: matrix, 384 × 329; field of view (FOV), 18 × 18 cm; number of slabs, 4; number of overlapped sections between two slabs, 11; flip angle, 18°; TR, 23 ms; TE, 2.9 ms; section thickness, 1.0 mm; number of excitations (NEX), 1; bandwidth, 31.25 kHz; and acquisition time, 6 min, 14 s. Those of silent MRA were as follows: matrix, 150 × 150; FOV, 18 × 18 cm; flip angle, 5°; TR, 799 ms; TE, 0.016 ms; section thickness, 1.2 mm; NEX, 1; bandwidth, 31.25 kHz; and acquisition time, 5 min, 29 s. The readout-sampling scheme in silent MRA was zero TE sequence by 3D radial sampling. The label method and duration have not been disclosed to the public, and we used silent MRA with default settings used in the previous studies [27]. The slice geometry of TOF-MRA and silent MRA were OM-line and axial plane, respectively. All MRA scans analyzed in the present study were performed within 2 months before or after DSA or 4D CTA.

DSA, 4D CTA technique

After catheterization of the internal carotid and the vertebral arteries via a femoral artery approach, diagnostic biplanar intra-arterial DSA (Inova; GE Healthcare, Milwaukee, Wisconsin, USA) was performed using automated injection of a contrast agent by a trained neurosurgeon. Temporal resolution of the images was 4 frames/s and 7.5 frames/s if necessary. 4D CTA was performed using a 320-slice scanner (Aquilion One; Canon Medical Systems, Otawara, Japan). To determine the optimal timing of dynamic scans, a test scan was performed using 20 mL contrast agent of 370 mg I/mL (iopamidol, Iopamiron 370; Bayer Yakihin, Osaka, Japan) at 5 mL/s, followed by 20 mL of saline, at the level of the carotid bulb. The 4D CTA scanning protocol consisted of a 11-s continuous acquisition (80 kV, 300 mAs, 0.5-s rotation speed) in the arterial to venous phase after a bolus injection of 50-mL contrast agent and 4-volume intermittent scans at a 4-s interval in the late venous phase.

Table 1 Visibility of cerebral AVM components on two types of MRA images

	TOF MRA (average score ± SD)	Interobserver agreement κ value	Silent MRA (average score ± SD)	Interobserver agreement κ value	*p* value
Feeder	3.21 ± 1.4	0.78	3.66 ± 1.32	0.72	0.22
Nidus	2.07 ± 0.84	0.62	4.24 ± 0.72	0.55	< 0.001
Drainer	1.86 ± 1.06	0.46	3.17 ± 1.47	0.66	< 0.001

TOF tight of flight, *SD* standard deviation

Image analysis

One neuroradiologist (22 years of experience) selected the cases which met the inclusion criteria for the reading study. Confirmation by means of DSA or 4D CTA was used as the reference standard for all the evaluations. With regard to the AVM detection and visualization, two experienced interventional neurosurgeons (both had 7-years experiences of DSA and MRI) independently reviewed TOF-MRA and silent MRA images on a PACS workstation. Disagreements were resolved by consensus. Three-dimensional maximum intensity projection (MIP) and source images were used for the interpretation of the MRA images. The order of images to be interpreted was TOF-MRA first, followed by silent MRA. The interval of readings between TOF-MRA and silent MRA was over at least 2 weeks. The observers were blinded to other imaging findings and clinical information. The criteria for a detection of AV shunt lesions on TOF-MRA and silent MRA images included the presence of hyperintense signal in areas of the nidus and/or drainer. Micro AVM was defined as the AVM with a nidus diameter less than 10 mm.

The observers independently graded the visualization of the feeder, nidus, and drainer of AVMs on TOF- and silent MRA images using a 5-point scale: Grade 1, not visible (no signal); Grade 2, poor (ambiguous visualization with severe blurring or artifacts); Grade 3, fair (moderate image quality with moderate blurring or artifacts); Grade 4, good (good image quality with slight blurring or artifacts); and Grade 5, excellent (sufficient image quality without artifacts).

Assessment of Spetzler–Martin grade by using TOF-MRA and silent MRA was independently performed by the two observers. Disagreements were resolved by consensus. CAVMs were characterized according to the Spetzler–Martin grading system [28]. The nidus size was classified as small (< 3 cm), medium (3–6 cm) or large (> 6 cm). Measurements were performed on source images of MRA. Location was

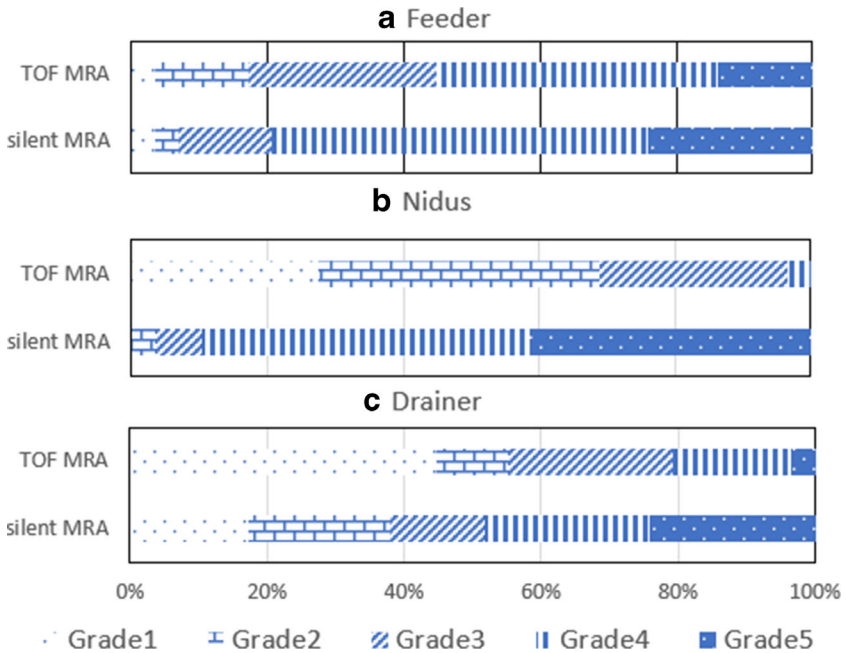

Fig. 1 Distribution of the image quality grade for feeder (**a**), nidus (**b**) and drainer (**c**) of AVM on TOF-MRA and silent MRA images. For feeders on both the MRA sequences, 80–90% were delineated with acceptable quality (Grades 3–5). The delineation with acceptable quality was obtained in about 95% of all niduses for Silent MRA, whereas it was 30% for TOF MRA. For drainers, the delineation with acceptable quality was seen in more than 60% of lesions for silent MRA and in only 30% for TOF MRA. Grade 1, not visible (no signal); Grade 2, poor (ambiguous visualization with severe blurring or artifacts); Grade 3, fair (moderate image quality with moderate blurring or artifacts); Grade 4, good (good image quality with slight blurring or artifacts); and Grade 5, excellent (sufficient image quality without artifacts)

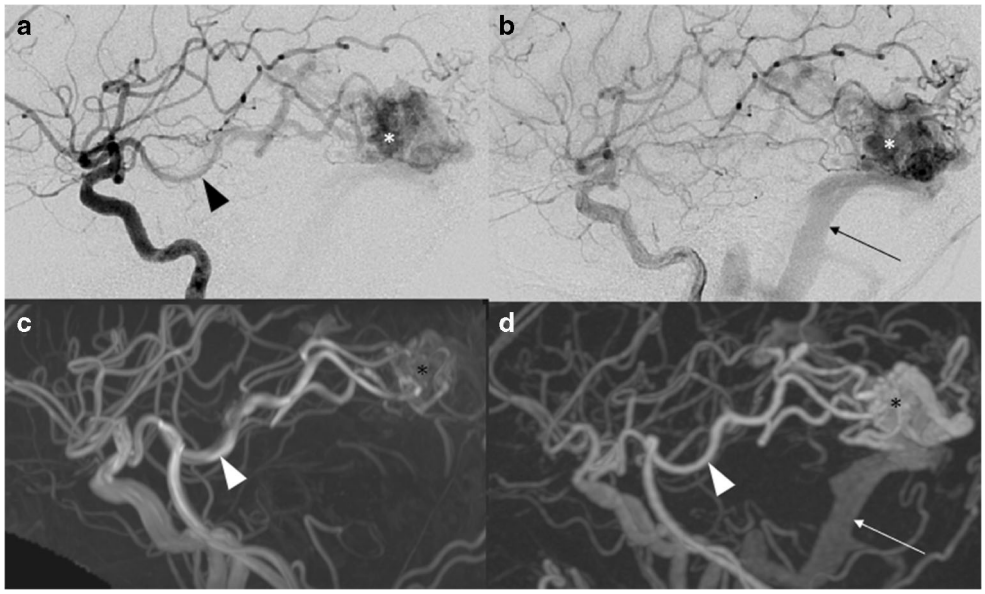

Fig. 2 DSA and MRA images of a 40-year-old woman with a left occipital CAVM. DSA (lateral projection from the left internal carotid artery) at arterial (**a**) and late arterial phases (**b**) reveals a AVM nidus (*) fed primarily by the left posterior cerebral artery (arrowhead) and its drainer (arrow). The nidus (asterisk) and drainer (arrow) are better delineated on Silent MRA images (**d**) than the TOF MRA ones (**c**) (arrows). The feeders were judged to be Grade 5 on TOF- (**c**) and Silent MRA images (**d**) by both observers. The drainers were judged to be Grade 2 on TOF- (**c**) and Grade 5 on silent MRA images (**d**)

categorized as being in an eloquent or non-eloquent area and venous drainage was categorized as superficial or deep. When both superficial and deep venous drainages were seen, it was classified as deep. In the assessment of Spetzler–Martin grade, T2-weighted MRI was also used as the standard reference.

After the blinded study, the structures of CAVMs on MRA images were reviewed retrospectively by the two observers in consensus, together with the clinical and angiographic findings.

Statistical analysis

The detectability of AV shunt lesions on TOF- and silent MRA images was calculated using DSA or 4D CTA as reference standards. The accuracy of Spetzler–Martin grading was compared between TOF-MRA and silent MRA. Fisher's exact test was performed to compare the accuracy between the results of TOF-MRA and those of silent MRA. To compare the mean visualization scores between the TOF-MRA and silent MRA, the Mann–Whitney U test was used. The level of interobserver agreement between the two readers with respect to the visualization of the AVM was determined by calculating the k coefficient ($k < 0.2$, poor; $0.21 < k < 0.40$, fair; $0.41 < k < 0.60$, moderate; $0.61 < k < 0.80$, good; $0.81 < k < 0.90$, very good; and $k > 0.90$, excellent agreement).The software R was used for all analyses [29], A p value of less than 0.05 was considered to indicate a statistically significant difference.

Results

For all 29 CAVMs, 23 (79%) lesions were detected for TOF-MRA (k = 1.0) and all (100%) for silent MRA (k = 1.0). Of 10 micro AVMs, only 4 (40%) lesions were detectable on TOF-MRA (k = 1.0) and all the lesions on silent MRA (k = 1.0). A significant difference in the detection rate of micro AVMs between the sequences was observed ($p < 0.01$).

Table 1 and Fig. 1 show the summary of the visualization score of the feeder, nidus, and drainer on TOF-MRA and silent MRA images. The mean score ± standard deviation of feeder,

Table 2 Visibility of micro AVM components on two types of MRA images

	TOF MRA (average score ± SD)	Interobserver agreement κ value	Silent MRA (average score ± SD)	Interobserver agreement κ value	p value
Feeder	1.8 ± 1.14	0.49	2.6 ± 0.84	0.57	0.08
Nidus	1.7 ± 0.95	0.62	3.9 ± 0.88	0.53	0.01
Drainer	1 ± 0	1	1.7 ± 0.67	0.57	< 0.001

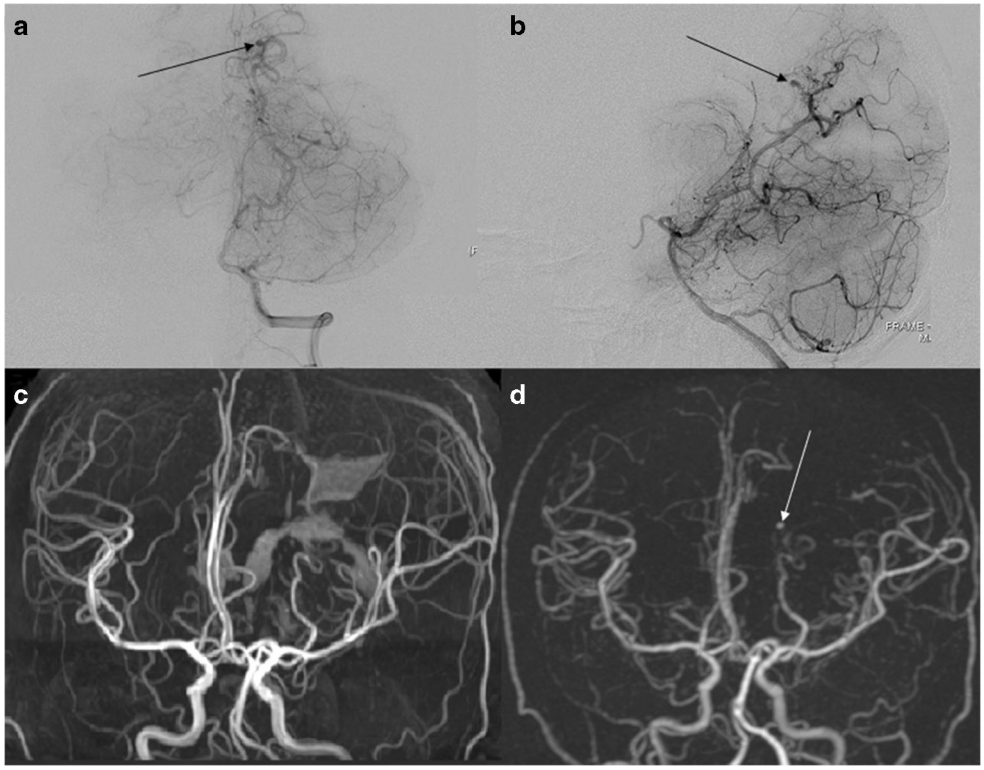

Fig. 3 DSA and MRA images of a 22-year-old woman with a micro AVM. Anteroposterior (**a**) and lateral (**b**) projection images of DSA from the left vertebral artery at late arterial phase reveals a micro AVM nidus (arrow) fed by a branch of the posterior cerebral artery. A micro AVM nidus is not visualized on TOF MRA (**c**) probably due to a hyperintense hematoma, while a tiny nidus (arrow) is visualized on silent MRA (**d**). According to both the observers, the nidus was judged as Grade 1 for TOF MRA (**c**) and Grade 5 for Silent MRA (**d**)

nidus, and drainer was 3.21 ± 1.44, 2.07 ± 164 0.84, and 1.86 ± 1.06 for TOF MRA and 3.66 ± 1.32, 4.24 ± 0.72, and 3.17 ± 1.47 for silent MRA, respectively. The mean score of the nidus and drainer was significantly higher for silent MRA than TOF-MRA ($p < 0.001$), while there was no significant difference in the feeder between the two sequences ($p = 0.22$) (Fig. 2). The interobserver agreement was moderate-to-good for both TOF-MRA and silent MRA (Table 1). The similar results were also found when assessing micro CAVMs (Table 2 and Fig. 3). The summary of the assessment of Spetzler–Martin grade by TOF-MRA and silent MRA is shown in Table 3. The accuracy of Spetzler–Martin grade for TOF-MRA and silent MRA were 11/29 (38%) and 23/29 (79.3%), respectively. There was a significant difference in the accuracy between the two types of MRA ($p < 0.001$).

As six micro CAVMs were not visualized on TOF MRA images, the exact size of the micro CAVMs was not able to measure. Apart from them, in 12 CAVMs, TOF-MRA did not demonstrate their drainers, which led to false classification in Spetzler–Martin grade. By contrast, silent MRA could not provide the correct information about eloquence in two small CAVMs on the source images. In addition, silent MRA could not depict their drainers in six cases with micro CAVM.

Discussion

This study revealed that the sensitivity for the detection of CAVMs and the visibility for nidus and draining veins were higher for silent MRA than TOF MRA. In addition, micro CAVMs, which were defined as a nidus size of less than 10 mm, were detected more effectively for silent MRA than TOF MRA.

TOF-MRA is sometimes insufficient to evaluate certain lesions because it has some characteristic artifacts [13, 14, 26]. Since silent MRA does not depend on the inflow effect

Table 3 Accuracy of each MRA with respect to the three parameters (size, eloquence, deep drainer) and the Spetzler–Martin Grade

	Cases (*N*)	TOF MRA (%)	Silent MRA (%)
Size (<3 cm, 3–6 cm, > 6 cm)	*N* = 19, 8, 2	68%, 100%, 100%	100%, 100%, 100%
Eloquence (no, yes)	*N* = 7,22	57%, 86%	71%, 100%
drainer (superficial, deep)	*N* = 26, 3	42%, 0%	77%, 100%
Spetzler–Martin Grade Accuracy rate		38% (11/29)	79.3% (23/29)

TOF tight of flight

into the imaging slab like TOF-MRA, it should be suitable to visualize complex flow in CAVMs. In addition, a high signal due to a hemorrhage is canceled out on silent MRA images owing to subtraction of the images acquired by labelling from those of the control. These effects must have affected our results. In ASL scans, without AV shunt lesions, such false positive lesions cannot be found because T1 dephasing of labeled water is shorter than the capillary transit time.

In the last decade, ASL-based MRI has provided abundant and practical information regarding cerebral AV shunt diseases [18–21, 23–26]. Recent development of using pseudocontinous spin labeling, fast imaging acquisitions, and three-dimensional radial sampling trajectories have enabled ASL-based MRA. Schubert et al. demonstrated the excellent sensitivity and specificity of 4D ASL MRA in detecting AV shunt lesions [24]. However, TE of 4D MRA is not as short as that of silent MRA. The blood flow signal indicting complex or turbulent flow in CAVMs could disappear in a short time. Therefore, 4D MRA may not provide clear visualization of nidus or draining veins, compared to silent MRA in which almost 0 TE can minimize phase dispersion in the labeled blood flow signal and reduce magnetic susceptibility artifacts.

Silent MRA may have several merits in neurosurgical clinical practice. Silent MRA has been reported to be effective to delineate aneurysms with stenting [27]. Based on our results, there may be several advantages in patients with CAVM. First, it may be a good screening method for cerebral AV shunt diseases. TOF-MRA cannot depict micro AVMs properly in many cases [30]. Actually, the sensitivity of TOF-MRA for detecting micro AVMs was only 40% in our study, while that of silent MRA was 100%. In specific diseases like hereditary hemorrhagic telangiectasia (HHT), micro or small AVMs are frequent [31]. Silent MRA may be useful for the screening tool. Second, silent MRA may be helpful for following up unstable AVMs. Certain AVMs dynamically change their structures on the venous side, such as varix formation and stenosis of the venous portion, which are risk factors for rupture and require an aggressive surgical policy [4–9]. Third, based on the relatively satisfactory accuracy of Spetzler–Martin grade assessment by silent MRA (around 80% in our result), it may help evaluate surgical risk of CAVM instead of other invasive modalities.

In the present study, there were several limitations. First, it may have included unforeseen bias because of its retrospective design. Second, no other ASL-based MRA techniques were included. Recently, such modalities have been reported to be effective in examining CAVMs [18–21, 23–26] Further comparative studies with other ASL-based MRA may be needed. Third, there was a difference in the spatial resolution between the two techniques. The scan time of the techniques was clinically acceptable. Fourth, our study population was relatively small. Further studies with a larger number of patients are needed to clarify the role of the technique in the clinical setting.

In conclusion, CAVM components, especially nidus and drainers, and micro AVM were visualized more clearly by silent MRA than by TOF-MRA. Silent MRA may be an effective screening and follow-up modality for CAVMs. Further studies are required to determine the clinical role of this technique.

Funding No funding was received for this study.

Compliance with ethical standards

Conflict of interest The authors declare that they have no conflict of interest.

Ethical approval All procedures performed in the studies involving human participants were in accordance with the ethical standards of the institutional and/or national research committee and with the 1964 Helsinki Declaration and its later amendments or comparable ethical standards.

Informed consent Our hospital IRB deemed informed consent unnecessary for this study.

References

1. Laakso A, Dashti R, Seppänen J, Juvela S, Väärt K, Niemelä M, Sankila R, Hernesniemi JA (2008) Long-term excess mortality in 623 patients with brain arteriovenous malformations. Neurosurgery 63(2):244–253
2. Michalak SM, Rolston JD, Lawton MT (2016) Incidence and predictors of complications and mortality in cerebrovascular surgery: national trends from 2007 to 2012. Neurosurgery 79(2):182–193
3. Mohr JP, Parides MK, Stapf C, Moquete E, Moy CS, Overbey JR, Al-Shahi Salman R, Vicaut E, Young WL, Houdart E, Cordonnier C, Stefani MA, Hartmann A, von Kummer R, Biondi A, Berkefeld J, Klijn CJ, Harkness K, Libman R, Barreau X, Moskowitz AJ, international ARUBA investigators (2014) Medical management with or without interventional therapy for unruptured brain arteriovenous malformations (ARUBA) a multicentre, non-blinded, randomised trial. Lancet 383(9917):614–621
4. Halim AX, Johnston SC, Singh V, McCulloch CE, Bennett JP, Achrol AS, Sidney S, Young WL (2014) Longitudinal risk of intracranial hemorrhage in patients with arteriovenous malformation of the brain within a defined population. Stroke 35:1697–1702
5. Hernesniemi JA, Dashti R, Juvela S, Väärt K, Niemelä M, Laakso A (2008) Natural history of brain arteriovenous malformations: a long-term follow-up study of risk of hemorrhage in 238 patients. Neurosurgery 63(5):823–829 discussion 829-31
6. Stapf C, Mast H, Sciacca RR, Choi JH, Khaw AV, Connolly ES, Pile-Spellman J, Mohr JP (2006) Predictors of hemorrhage in patients with untreated brain arteriovenous malformation. Neurology 9;66(9):1350–1355
7. Meisel HJ, Mansmann U, Alvarez H, Rodesch G, Brock M, Lasjaunias P (2000) Cerebral arteriovenous malformations and associated aneurysms:analysis of 305 cases from a series of 662 patients. Neurosurgery 46:793–802
8. Mast H, Young WL, Koennecke HC, Sciacca RR, Osipov A, Pile-Spellman J, Hacein-Bey L, Duong H, Stein BM, Mohr JP (1997)

Risk of spontaneous haemorrhage after diagnosis of cerebral arteriovenous malformation. Lancet 350:1065–1068
9. Stapf C, Mohr JP, Sciacca RR, Hartmann A, Aagaard BD, Pile-Spellman J, Mast H (2000) Incident hemorrhage risk of brain arteriovenous malformations located in the arterial borderzones. Stroke 31:2365–2368
10. Thiex R, Norbash AM, Frerichs KU (2010) The safety of dedicated-team catheter-based diagnostic cerebral angiography in the era of advanced noninvasive imaging. AJNR Am J Neuroradiol 31:230–234
11. Willinsky RA, Taylor SM, TerBrugge K, Farb RI, Tomlinson G, Montanera W (2003) Neurologic complications of cerebral angiography: prospective analysis of 2,899 procedures and review of the literature. Radiology 227:522–528
12. Dawkins AA, Evans AL, Wattam J, Romanowski CA, Connolly DJ, Hodgson TJ, Coley SC (2007) Complications of cerebral angiography: a prospective analysis of 2,924 consecutive procedures. Neuroradiology 49:753–759
13. Buis DR, Bot JC, Barkhof F, Knol DL, Lagerwaard FJ, Slotman BJ, Vandertop WP, van den Berg R (2012) The predictive value of 3D time-of-flight MR angiography in assessment of brain arteriovenous malformation obliteration after radiosurgery. AJNR Am J Neuroradiol 33(2):232–238
14. Farb RI, McGregor C, Kim JK, Laliberte M, Derbyshire JA, Willinsky RA, Cooper PW, Westman DG, Cheung G, Schwartz ML, Stainsby JA, Wright GA (2001) Intracranial arteriovenous malformations: real-time auto-triggered elliptic centric-ordered 3D gadolinium-enhanced MR angiography–initial assessment. Radiology 220(1):244–251
15. Willemse RB, Mager JJ, Westermann CJ, Overtoom TT, Mauser H, Wolbers JG (2000) Bleeding risk of cerebrovascular malformations in hereditary hemorrhagic telangiectasia. J Neurosurg 92(5):779–784
16. Meybodi AT, Kim H, Nelson J, Hetts SW, Krings T, ter Brugge KG, Faughnan ME, Lawton MT, On Behalf Of The Brain Vascular Malformation Consortium HHT Investigator Group (2018) Surgical treatment vs nonsurgical treatment for brain arteriovenous malformations in patients with hereditary hemorrhagic telangiectasia: a retrospective multicenter consortium study. Neurosurgery 82(1):35–47
17. Alibek S, Vogel M, Sun W, Winkler D, Baker CA, Burke M, Gloger H (2014) Acoustic noise reduction in MRI using silent scan: an initial experience. Diagn Interv Radiol 20(4):360–363
18. Iryo Y, Hirai T, Nakamura M, Kawano T, Kaku Y, Ohmori Y, Kai Y, Azuma M, Nishimura S, Shigematsu Y, Kitajima M, Yamashita Y (2016) Evaluation of intracranial arteriovenous malformations with four-dimensional arterial-spin labeling-based 3-T magnetic resonance angiography. J Comput Assist Tomogr 40:290–296
19. Xu J, Shi D, Chen C, Li Y, Wang M, Han X, Jin L, Bi X (2011) Noncontrast-enhanced four-dimensional MR angiography for the evaluation of cerebral arteriovenous malformation: a preliminary trial. J Magn Reson Imaging 34:1199–1205
20. Raoult H, Bannier E, Robert B, Barillot C, Schmitt P, Gauvrit JY (2014) Time-resolved spin-labeled MR angiography for the depiction of cerebral arteriovenous malformations: a comparison of techniques. Radiology 271:524–533
21. Wolf RL, Wang J, Detre JA, Zager EL, Hurst RW (2008) Arteriovenous shunt visualization in arteriovenous malformations with arterial spin-labeling MR imaging. AJNR Am J Neuroradiol 29:681–687
22. Yu S, Yan L, Yao Y, Wang S, Yang M, Wang B, Zhuo Y, Ai L, Miao X, Zhao J, Wang DJ (2012) Noncontrast dynamic MRA in intracranial arteriovenous malformation (AVM), comparison with time of flight (TOF) and digital subtraction angiography (DSA). Magn Reson Imaging 30(6):869–877
23. Amukotuwa SA, Heit JJ, Marks MP, Fischbein N, Bammer R (2016) Detection of cortical venous drainage and determination of the Borden type of dural arteriovenous fistula by means of 3D pseudocontinuous arterial spin-labeling MRI. AJR Am J Roentgenol 207:163–169
24. Le TT, Fischbein NJ, André JB, Wijman C, Rosenberg J, Zaharchuk G (2012) Identification of venous signal on arterial spin labeling improves diagnosis of dural arteriovenous fistulas and small arteriovenous malformations. AJNR Am J Neuroradiol 33:61–68
25. Schubert T, Clark Z, Sandoval-Garcia C, Zea R, Wieben O, Wu H, Turski PA, Johnson KM (2018) Non contrast, pseudo-continuous arterial spin labeling and accelerated 3-dimensional radial acquisition intracranial 3-dimensional magnetic resonance angiography for the detection and classification of intracranial arteriovenous shunts. Investig Radiol 53(2):80–86
26. Kukuk GM, Hadizadeh DR, Boström A, Gieseke J, Bergener J, Nelles M, Mürtz P, Urbach H, Schild HH, Willinek WA (2010) Cerebral arteriovenous malformations at 3.0 T: intraindividual comparative study of 4D-MRA in combination with selective arterial spin labeling and digital subtraction angiography. Investig Radiol 45:126–132
27. Takano N, Suzuki M, Irie R, Yamamoto M, Teranishi K, Yatomi K, Hamasaki N, Kumamaru KK, Hori M, Oishi H, Aoki S (2017) Non-contrast-enhanced silent scan MR angiography of intracranial anterior circulation aneurysms treated with a low-profile visualized intraluminal support device. AJNR Am J Neuroradiol 38(8):1610–1616
28. Spetzler RF, Martin NA (1986) A proposed grading system for arteriovenous malformations. J Neurosurg 65:476–483
29. The Comprehensive R Archive Network. The R Project for Statistical Computing. https://cran.r-project.org/ Published 2017. Accessed December 13, 2018
30. Mukherji SK, Quisling RG, Kubilis PS, Finn JP, Friedman WA (1995) Intracranial arteriovenous malformations: quantitative analysis of magnitude contrast MR angiography versus gradient-echo MR imaging versus conventional angiography. Radiology 196(1):187–193
31. Matsubara S, Mandzia JL, terBrugge K, Willinsky RA, Faughnan ME (2000) Angiographic and clinical characteristics of patients with cerebral arteriovenous malformations associated with hereditary hemorrhagic telangiectasia. AJNR Am J Neuroradiol 21(6):1016–1020